Measurement of Trilinear Gauge Couplings in e^+e^- Collisions at 161 GeV and 172 GeV

P. Abreu, W. Adam, T. Adye, P. Adzic, G D. Alekseev, R. Alemany, P P. Allport, S. Almehed, U. Amaldi, S. Amato, et al.

EUROPEAN ORGANIZATION FOR NUCLEAR RESEARCH

CERN–PPE/97–163

17 December 1997

Measurement of Trilinear Gauge Couplings in e^+e^- Collisions at 161 GeV and 172 GeV

DELPHI Collaboration

Abstract

Trilinear gauge boson couplings are measured using data taken by DELPHI at 161 GeV and 172 GeV. Values for WWV couplings ($V = Z, \gamma$) are determined from a study of the reactions $e^+e^- \to W^+W^-$ and $e^+e^- \to We\nu$, using differential distributions from the WW final state in which one W decays hadronically and the other leptonically, and total cross-section data from other channels. Limits are also derived on neutral $ZV\gamma$ couplings from an analysis of the reaction $e^+e^- \to \gamma$ + invisible particles.

(Submitted to Phys. Lett. B)

P.Abreu[21], W.Adam[49], T.Adye[36], P.Adzic[11], G.D.Alekseev[16], R.Alemany[48], P.P.Allport[22], S.Almehed[24], U.Amaldi[9], S.Amato[46], P.Andersson[43], A.Andreazza[9], P.Antilogus[25], W-D.Apel[17], Y.Arnoud[14], B.Åsman[43], J-E.Augustin[25], A.Augustinus[9], P.Baillon[9], P.Bambade[19], F.Barao[21], R.Barbier[25], D.Y.Bardin[16], G.Barker[9], A.Baroncelli[39], O.Barring[24], M.J.Bates[36], M.Battaglia[15], M.Baubillier[23], K-H.Becks[51], M.Begalli[6], P.Beilliere[8], Yu.Belokopytov[9,52], A.C.Benvenuti[5], C.Berat[14], M.Berggren[25], D.Bertini[25], D.Bertrand[2], M.Besancon[38], F.Bianchi[44], M.Bigi[44], M.S.Bilenky[16], P.Billoir[23], M-A.Bizouard[19], D.Bloch[10], M.Bonesini[27], W.Bonivento[27], M.Boonekamp[38], P.S.L.Booth[22], A.W.Borgland[4], G.Borisov[38], C.Bosio[39], O.Botner[47], E.Boudinov[30], B.Bouquet[19], C.Bourdarios[19], T.J.V.Bowcock[22], I.Bozovic[11], M.Bozzo[13], P.Branchini[39], K.D.Brand[35], T.Brenke[51], R.A.Brenner[47], R.Brown[9], P.Bruckman[35], J-M.Brunet[8], L.Bugge[32], T.Buran[32], T.Burgsmueller[51], P.Buschmann[51], S.Cabrera[48], M.Caccia[27], M.Calvi[27], A.J.Camacho Rozas[40], T.Camporesi[9], V.Canale[37], M.Canepa[13], F.Carena[9], L.Carroll[22], C.Caso[13], M.V.Castillo Gimenez[48], A.Cattai[9], F.R.Cavallo[5], Ch.Cerruti[10], V.Chabaud[9], M.Chapkin[41], Ph.Charpentier[9], L.Chaussard[25], P.Checchia[35], G.A.Chelkov[16], M.Chen[2], R.Chierici[44], P.Chliapnikov[41], P.Chochula[7], V.Chorowicz[25], J.Chudoba[29], P.Collins[9], M.Colomer[48], R.Contri[13], E.Cortina[48], G.Cosme[19], F.Cossutti[9], J-H.Cowell[22], H.B.Crawley[1], D.Crennell[36], G.Crosetti[13], J.Cuevas Maestro[33], S.Czellar[15], B.Dalmagne[19], G.Damgaard[28], P.D.Dauncey[36], M.Davenport[9], W.Da Silva[23], A.Deghorain[2], G.Della Ricca[45], P.Delpierre[26], N.Demaria[9], A.De Angelis[9], W.De Boer[17], S.De Brabandere[2], C.De Clercq[2], C.De La Vaissiere[23], B.De Lotto[45], A.De Min[35], L.De Paula[46], H.Dijkstra[9], L.Di Ciaccio[37], A.Di Diodato[37], A.Djannati[8], J.Dolbeau[8], K.Doroba[50], M.Dracos[10], J.Drees[51], K.-A.Drees[51], M.Dris[31], A.Duperrin[25], J-D.Durand[25,9], D.Edsall[1], R.Ehret[17], G.Eigen[4], T.Ekelof[47], G.Ekspong[43], M.Ellert[47], M.Elsing[9], J-P.Engel[10], B.Erzen[42], M.Espirito Santo[21], E.Falk[24], G.Fanourakis[11], D.Fassouliotis[45], J.Fayot[23], M.Feindt[17], P.Ferrari[27], A.Ferrer[48], S.Fichet[23], A.Firestone[1], P.-A.Fischer[9], U.Flagmeyer[51], H.Foeth[9], E.Fokitis[31], F.Fontanelli[13], F.Formenti[9], B.Franek[36], A.G.Frodesen[4], R.Fruhwirth[49], F.Fulda-Quenzer[19], J.Fuster[48], A.Galloni[22], D.Gamba[44], M.Gandelman[46], C.Garcia[48], J.Garcia[40], C.Gaspar[9], M.Gaspar[46], U.Gasparini[35], Ph.Gavillet[9], E.N.Gazis[31], D.Gele[10], J-P.Gerber[10], L.Gerdyukov[41], N.Ghodbane[25], F.Glege[51], R.Gokieli[50], B.Golob[42], P.Goncalves[21], I.Gonzalez Caballero[40], G.Gopal[36], L.Gorn[1,53], M.Gorski[50], Yu.Gouz[41], V.Gracco[13], J.Grahl[1], E.Graziani[39], C.Green[22], A.Grefrath[51], P.Gris[38], G.Grosdidier[19], K.Grzelak[50], M.Gunther[47], J.Guy[36], F.Hahn[9], S.Hahn[51], S.Haider[9], Z.Hajduk[18], A.Hallgren[47], K.Hamacher[51], F.J.Harris[34], V.Hedberg[24], S.Heising[17], R.Henriques[21], J.J.Hernandez[48], P.Herquet[2], H.Herr[9], T.L.Hessing[34], J.-M.Heuser[51], E.Higon[48], S-O.Holmgren[43], P.J.Holt[34], D.Holthuizen[30], S.Hoorelbeke[2], M.Houlden[22], J.Hrubec[49], K.Huet[2], K.Hultqvist[43], J.N.Jackson[22], R.Jacobsson[43], P.Jalocha[9], R.Janik[7], Ch.Jarlskog[24], G.Jarlskog[24], P.Jarry[38], B.Jean-Marie[19], E.K.Johansson[43], L.Jonsson[24], P.Jonsson[24], C.Joram[9], P.Juillot[10], F.Kapusta[23], K.Karafasoulis[11], S.Katsanevas[25], E.C.Katsoufis[31], R.Keranen[4], B.A.Khomenko[16], N.N.Khovanski[16], B.King[22], N.J.Kjaer[30], O.Klapp[51], H.Klein[9], P.Kluit[30], D.Knoblauch[17], P.Kokkinias[11], M.Koratzinos[9], K.Korcyl[18], V.Kostioukhine[41], C.Kourkoumelis[3], O.Kouznetsov[16], M.Krammer[49], C.Kreuter[9], I.Kronkvist[24], Z.Krumstein[16], P.Kubinec[7], W.Kucewicz[18], K.Kurvinen[15], C.Lacasta[9], J.W.Lamsa[1], L.Lanceri[45], D.W.Lane[1], P.Langefeld[51], V.Lapin[41], J-P.Laugier[38], R.Lauhakangas[15], G.Leder[49], F.Ledroit[14], V.Lefebure[2], C.K.Legan[1], A.Leisos[11], R.Leitner[29], J.Lemonne[2], G.Lenzen[51], V.Lepeltier[19], T.Lesiak[18], M.Lethuillier[38], J.Libby[34], D.Liko[9], A.Lipniacka[43], I.Lippi[35], B.Loerstad[24], J.G.Loken[34], J.H.Lopes[46], J.M.Lopez[40], D.Loukas[11], P.Lutz[38], L.Lyons[34], J.MacNaughton[49], J.R.Mahon[6], A.Maio[21], A.Malek[51], T.G.M.Malmgren[43], V.Malychev[16], F.Mandl[49], J.Marco[40], R.Marco[40], B.Marechal[46], M.Margoni[35], J-C.Marin[9], C.Mariotti[9], A.Markou[11], C.Martinez-Rivero[33], F.Martinez-Vidal[48], S.Marti i Garcia[22], F.Matorras[40], C.Matteuzzi[27], G.Matthiae[37], F.Mazzucato[35], M.Mazzucato[35], M.Mc Cubbin[22], R.Mc Kay[1], R.Mc Nulty[9], G.Mc Pherson[22], J.Medbo[47], C.Meroni[27], W.T.Meyer[1], M.Michelotto[35], E.Migliore[44], L.Mirabito[25], W.A.Mitaroff[49], U.Mjoernmark[24], T.Moa[43], R.Moeller[28], K.Moenig[9], M.R.Monge[13], X.Moreau[23], P.Morettini[13], K.Muenich[51], M.Mulders[30], L.M.Mundim[6], W.J.Murray[36], B.Muryn[14,18], G.Myatt[34], T.Myklebust[32], F.Naraghi[14], F.L.Navarria[5], S.Navas[48], K.Nawrocki[50], P.Negri[27], S.Nemecek[12], N.Neufeld[9], W.Neumann[51], N.Neumeister[49], R.Nicolaidou[14], B.S.Nielsen[28], M.Nieuwenhuizen[30], V.Nikolaenko[10], M.Nikolenko[10,16], P.Niss[43], A.Nomerotski[35], A.Normand[22], A.Nygren[24], W.Oberschulte-Beckmann[17], V.Obraztsov[41], A.G.Olshevski[16], A.Onofre[21], R.Orava[15], G.Orazi[10], K.Osterberg[15], A.Ouraou[38], P.Paganini[19], M.Paganoni[27], S.Paiano[5], R.Pain[23], R.Paiva[21], H.Palka[18], Th.D.Papadopoulou[31], K.Papageorgiou[11], L.Pape[9], C.Parkes[34], F.Parodi[13], U.Parzefall[22], A.Passeri[39], M.Pegoraro[35], H.Pernegger[49], M.Pernicka[49], A.Perrotta[5], C.Petridou[45], A.Petrolini[13], H.T.Phillips[36], G.Piana[13], F.Pierre[38], M.Pimenta[21], E.Piotto[35], T.Podobnik[34], O.Podobrin[9], M.E.Pol[6], G.Polok[18], P.Poropat[45], V.Pozdniakov[16], P.Privitera[37], N.Pukhaeva[16], A.Pullia[27], D.Radojicic[34], S.Ragazzi[27], H.Rahmani[31], J.Rames[12], P.N.Ratoff[20], A.L.Read[32], P.Rebecchi[9], N.G.Redaelli[27], M.Regler[49], D.Reid[9], R.Reinhardt[51], P.B.Renton[34], L.K.Resvanis[3], F.Richard[19], J.Ridky[12], G.Rinaudo[44], O.Rohne[32], A.Romero[44], P.Ronchese[35], E.I.Rosenberg[1], P.Rosinsky[7], P.Roudeau[19], T.Rovelli[5], V.Ruhlmann-Kleider[38], A.Ruiz[40], H.Saarikko[15], Y.Sacquin[38], A.Sadovsky[16], G.Sajot[14], J.Salt[48], D.Sampsonidis[11], M.Sannino[13], H.Schneider[17], U.Schwickerath[17], M.A.E.Schyns[51], F.Scuri[45], P.Seager[20], Y.Sedykh[16], A.M.Segar[34], R.Sekulin[36], V.Senko[41], R.C.Shellard[6], A.Sheridan[22], R.Silvestre[38], F.Simonetto[35], A.N.Sisakian[16], T.B.Skaali[32], G.Smadja[25], N.Smirnov[41], O.Smirnova[24], G.R.Smith[36], O.Solovianov[41], A.Sopczak[17], R.Sosnowski[50], D.Souza-Santos[6], T.Spassov[21], E.Spiriti[39], P.Sponholz[51], S.Squarcia[13], D.Stampfer[9], C.Stanescu[39], S.Stanic[42], S.Stapnes[32], I.Stavitski[35], K.Stevenson[34], A.Stocchi[19], J.Strauss[49], R.Strub[10], B.Stugu[4], M.Szczekowski[50], M.Szeptycka[50], T.Tabarelli[27], O.Tchikilev[41], F.Tegenfeldt[47], F.Terranova[27], J.Thomas[34], A.Tilquin[26], J.Timmermans[30],

L.G.Tkatchev[16], T.Todorov[10], S.Todorova[10], D.Z.Toet[30], A.Tomaradze[2], B.Tome[21], A.Tonazzo[27], L.Tortora[39], G.Transtromer[24], D.Treille[9], G.Tristram[8], A.Trombini[19], C.Troncon[27], A.Tsirou[9], M-L.Turluer[38], I.A.Tyapkin[16], M.Tyndel[36], S.Tzamarias[11], B.Ueberschaer[51], O.Ullaland[9], V.Uvarov[41], G.Valenti[5], E.Vallazza[45], G.W.Van Apeldoorn[30], P.Van Dam[30], W.K.Van Doninck[2], J.Van Eldik[30], A.Van Lysebetten[2], I.Van Vulpen[30], N.Vassilopoulos[34], G.Vegni[27], L.Ventura[35], W.Venus[36], F.Verbeure[2], M.Verlato[35], L.S.Vertogradov[16], V.Verzi[37], D.Vilanova[38], P.Vincent[23], N.Vishnevsky[41], L.Vitale[45], E.Vlasov[41], A.S.Vodopyanov[16], V.Vrba[12], H.Wahlen[51], C.Walck[43], F.Waldner[45], C.Weiser[17], A.M.Wetherell[9], D.Wicke[51], J.H.Wickens[2], G.R.Wilkinson[9], W.S.C.Williams[34], M.Winter[10], M.Witek[18], T.Wlodek[19], G.Wolf[9], J.Yi[1], O.Yushchenko[41], A.Zalewska[18], P.Zalewski[50], D.Zavrtanik[42], E.Zevgolatakos[11], N.I.Zimin[16], G.C.Zucchelli[43], G.Zumerle[35]

[1] Department of Physics and Astronomy, Iowa State University, Ames IA 50011-3160, USA
[2] Physics Department, Univ. Instelling Antwerpen, Universiteitsplein 1, BE-2610 Wilrijk, Belgium
and IIHE, ULB-VUB, Pleinlaan 2, BE-1050 Brussels, Belgium
and Faculté des Sciences, Univ. de l'Etat Mons, Av. Maistriau 19, BE-7000 Mons, Belgium
[3] Physics Laboratory, University of Athens, Solonos Str. 104, GR-10680 Athens, Greece
[4] Department of Physics, University of Bergen, Allégaten 55, NO-5007 Bergen, Norway
[5] Dipartimento di Fisica, Università di Bologna and INFN, Via Irnerio 46, IT-40126 Bologna, Italy
[6] Centro Brasileiro de Pesquisas Físicas, rua Xavier Sigaud 150, BR-22290 Rio de Janeiro, Brazil
and Depto. de Física, Pont. Univ. Católica, C.P. 38071 BR-22453 Rio de Janeiro, Brazil
and Inst. de Física, Univ. Estadual do Rio de Janeiro, rua São Francisco Xavier 524, Rio de Janeiro, Brazil
[7] Comenius University, Faculty of Mathematics and Physics, Mlynska Dolina, SK-84215 Bratislava, Slovakia
[8] Collège de France, Lab. de Physique Corpusculaire, IN2P3-CNRS, FR-75231 Paris Cedex 05, France
[9] CERN, CH-1211 Geneva 23, Switzerland
[10] Institut de Recherches Subatomiques, IN2P3 - CNRS/ULP - BP20, FR-67037 Strasbourg Cedex, France
[11] Institute of Nuclear Physics, N.C.S.R. Demokritos, P.O. Box 60228, GR-15310 Athens, Greece
[12] FZU, Inst. of Phys. of the C.A.S. High Energy Physics Division, Na Slovance 2, CZ-180 40, Praha 8, Czech Republic
[13] Dipartimento di Fisica, Università di Genova and INFN, Via Dodecaneso 33, IT-16146 Genova, Italy
[14] Institut des Sciences Nucléaires, IN2P3-CNRS, Université de Grenoble 1, FR-38026 Grenoble Cedex, France
[15] Helsinki Institute of Physics, HIP, P.O. Box 9, FI-00014 Helsinki, Finland
[16] Joint Institute for Nuclear Research, Dubna, Head Post Office, P.O. Box 79, RU-101 000 Moscow, Russian Federation
[17] Institut für Experimentelle Kernphysik, Universität Karlsruhe, Postfach 6980, DE-76128 Karlsruhe, Germany
[18] Institute of Nuclear Physics and University of Mining and Metalurgy, Ul. Kawiory 26a, PL-30055 Krakow, Poland
[19] Université de Paris-Sud, Lab. de l'Accélérateur Linéaire, IN2P3-CNRS, Bât. 200, FR-91405 Orsay Cedex, France
[20] School of Physics and Chemistry, University of Lancaster, Lancaster LA1 4YB, UK
[21] LIP, IST, FCUL - Av. Elias Garcia, 14-1^{o}, PT-1000 Lisboa Codex, Portugal
[22] Department of Physics, University of Liverpool, P.O. Box 147, Liverpool L69 3BX, UK
[23] LPNHE, IN2P3-CNRS, Univ. Paris VI et VII, Tour 33 (RdC), 4 place Jussieu, FR-75252 Paris Cedex 05, France
[24] Department of Physics, University of Lund, Sölvegatan 14, SE-223 63 Lund, Sweden
[25] Université Claude Bernard de Lyon, IPNL, IN2P3-CNRS, FR-69622 Villeurbanne Cedex, France
[26] Univ. d'Aix - Marseille II - CPP, IN2P3-CNRS, FR-13288 Marseille Cedex 09, France
[27] Dipartimento di Fisica, Università di Milano and INFN, Via Celoria 16, IT-20133 Milan, Italy
[28] Niels Bohr Institute, Blegdamsvej 17, DK-2100 Copenhagen Ø, Denmark
[29] NC, Nuclear Centre of MFF, Charles University, Areal MFF, V Holesovickach 2, CZ-180 00, Praha 8, Czech Republic
[30] NIKHEF, Postbus 41882, NL-1009 DB Amsterdam, The Netherlands
[31] National Technical University, Physics Department, Zografou Campus, GR-15773 Athens, Greece
[32] Physics Department, University of Oslo, Blindern, NO-1000 Oslo 3, Norway
[33] Dpto. Fisica, Univ. Oviedo, Avda. Calvo Sotelo s/n, ES-33007 Oviedo, Spain, (CICYT-AEN96-1681)
[34] Department of Physics, University of Oxford, Keble Road, Oxford OX1 3RH, UK
[35] Dipartimento di Fisica, Università di Padova and INFN, Via Marzolo 8, IT-35131 Padua, Italy
[36] Rutherford Appleton Laboratory, Chilton, Didcot OX11 OQX, UK
[37] Dipartimento di Fisica, Università di Roma II and INFN, Tor Vergata, IT-00173 Rome, Italy
[38] DAPNIA/Service de Physique des Particules, CEA-Saclay, FR-91191 Gif-sur-Yvette Cedex, France
[39] Istituto Superiore di Sanità, Ist. Naz. di Fisica Nucl. (INFN), Viale Regina Elena 299, IT-00161 Rome, Italy
[40] Instituto de Fisica de Cantabria (CSIC-UC), Avda. los Castros s/n, ES-39006 Santander, Spain,
(CICYT-AEN96-1681)
[41] Inst. for High Energy Physics, Serpukov P.O. Box 35, Protvino, (Moscow Region), Russian Federation
[42] J. Stefan Institute, Jamova 39, SI-1000 Ljubljana, Slovenia and Department of Astroparticle Physics, School of
Environmental Sciences, Kostanjeviska 16a, Nova Gorica, SI-5000 Slovenia,
and Department of Physics, University of Ljubljana, SI-1000 Ljubljana, Slovenia
[43] Fysikum, Stockholm University, Box 6730, SE-113 85 Stockholm, Sweden
[44] Dipartimento di Fisica Sperimentale, Università di Torino and INFN, Via P. Giuria 1, IT-10125 Turin, Italy
[45] Dipartimento di Fisica, Università di Trieste and INFN, Via A. Valerio 2, IT-34127 Trieste, Italy
and Istituto di Fisica, Università di Udine, IT-33100 Udine, Italy
[46] Univ. Federal do Rio de Janeiro, C.P. 68528 Cidade Univ., Ilha do Fundão BR-21945-970 Rio de Janeiro, Brazil
[47] Department of Radiation Sciences, University of Uppsala, P.O. Box 535, SE-751 21 Uppsala, Sweden
[48] IFIC, Valencia-CSIC, and D.F.A.M.N., U. de Valencia, Avda. Dr. Moliner 50, ES-46100 Burjassot (Valencia), Spain
[49] Institut für Hochenergiephysik, Österr. Akad. d. Wissensch., Nikolsdorfergasse 18, AT-1050 Vienna, Austria
[50] Inst. Nuclear Studies and University of Warsaw, Ul. Hoza 69, PL-00681 Warsaw, Poland
[51] Fachbereich Physik, University of Wuppertal, Postfach 100 127, DE-42097 Wuppertal, Germany
[52] On leave of absence from IHEP Serpukhov
[53] Now at University of Florida

1 Introduction

One of the most important consequences of the $SU(2)\times U(1)$ symmetry of the Standard Model is the existence of non-Abelian self-couplings of the gauge bosons γ, W and Z^0. Using data taken in the DELPHI detector at LEP in 1996 at centre-of-mass energies of 161 and 172 GeV, events from the reactions $e^+e^-\rightarrow\ W^+W^-$ and $e^+e^-\rightarrow We\nu$ have been used to study WWV couplings, where $V\equiv Z,\gamma$. The reaction $e^+e^-\rightarrow\gamma\ +$ invisible particles has been used to study couplings at the $ZV\gamma$ vertex.

The WWV coupling arises in WW production through the diagrams involving s-channel exchange of Z^0 or γ. In single W production, the dominant amplitude involving a trilinear gauge coupling (TGC) is that arising from radiation of a virtual photon from the incident electron or positron. The Standard Model predicts a charge coupling, described by a parameter g_1^V in an effective WWV Lagrangian $\mathcal{L}_{WWV}$, and a dipole coupling κ_V, with $g_1^V\ =\ \kappa_V\ =\ 1$ [1]. In a general Lorentz-invariant description of the WWV interaction, other couplings, both CP-conserving and CP-violating, are possible, but their contributions are predicted to be zero in the Standard Model.

In searching for the presence of new physics, contributions from gauge-invariant operators of lowest dimension (≤ 6) have been considered, taking only those which have not been excluded by previous measurements. This leads to possible contributions $\alpha_{W\phi}$, $\alpha_{B\phi}$ and α_W from CP-conserving operators and $\tilde{\alpha}_{BW}$ and $\tilde{\alpha}_W$ from CP-violating operators. The CP-conserving parameters are related to the charge and dipole couplings defined above and to the quadrupole couplings λ_V in $\mathcal{L}_{WWV}$ by: $\Delta g_1^Z=\frac{\alpha_{W\phi}}{c_w^2}$, $\Delta\kappa_\gamma=\alpha_{W\phi}+\alpha_{B\phi}$, $\Delta\kappa_Z=\alpha_{W\phi}-\frac{s_w^2}{c_w^2}\alpha_{B\phi}$ and $\lambda_\gamma=\lambda_Z=\alpha_W$, where s_w and c_w are the sine and cosine of the electroweak mixing angle and Δg_1^Z, $\Delta\kappa_\gamma$ and $\Delta\kappa_Z$ represent deviations from Standard Model values [1]. Similarly, the CP-violating parameters are related to the relevant terms in $\mathcal{L}_{WWV}$ by: $\tilde{\kappa}_\gamma=\tilde{\alpha}_{BW}$, $\tilde{\kappa}_Z=\frac{s_w^2}{c_w^2}\tilde{\alpha}_{BW}$ and $\tilde{\lambda}_\gamma=\tilde{\lambda}_Z=\tilde{\alpha}_W$ [2].

The process $e^+e^-\rightarrow\gamma\ +$ invisible particles is described within the Standard Model by the radiative production of neutrino-antineutrino pairs, $e^+e^-\ \rightarrow\ \nu\bar{\nu}\gamma$. A W fusion diagram, containing a $WW\gamma$ coupling, also contributes to $\nu\bar{\nu}\gamma$ production, but its amplitude is very small at LEP2 energies, and its relative contribution is negligible [3]. Possible new physics contributions to single photon production could come from new families of neutrinos, from the radiative production of any other neutral weakly interacting particle, or from the s-channel exchange of γ or Z leading to $Z\gamma$ production via a triple vector boson coupling. In this paper the latter possibility is examined. The $ZV\gamma$ vertex has been described by Baur and Berger [4] in terms of a vertex function involving four independent terms $h_{1..4}^V$; in the Standard Model all of these are zero at tree level. The parameters are normally described by a form factor representation, $h_i^V(s)=h_{i0}^V/(1+s/\Lambda^2)^n$, with an energy Λ representing the scale at which a novel interaction would become manifest, and with a sufficiently large power n to ensure unitarity conservation at high energy. Conventionally, $n=3$ is used for $h_{1,3}^V$ and $n=4$ for $h_{2,4}^V$. The terms in h_1 and h_2 are CP-violating, and those in h_3 and h_4 CP-conserving. However, the minimum dimensionality of gauge-invariant operators contributing to $\mathcal{L}_{ZV\gamma}$ is 8 [5], so the observation of deviations from Standard Model predictions is *a priori* less likely in this channel than in those involving WWV couplings.

Results on WWV couplings have previously been reported in $\bar{p}p$ experiments [6–8], and in first reports of results at LEP2 [9,10]. Limits on $ZV\gamma$ couplings have been determined in $\bar{p}p$ experiments [6,8,11,12] and from LEP data taken at the Z^0 [13] and at 130-136 GeV [14].

The next section of this paper describes the selection of events from the data and the simulation of the various channels involved in the analysis. Results on the trilinear gauge coupling parameters describing the WWV and $ZV\gamma$ vertices are reported in sections 3 and 4, respectively, and a summary is given in section 5.

2 Event selection and simulation

In 1996, DELPHI recorded integrated luminosities of 10.0 pb^{-1} and 9.98 pb^{-1} at centre-of-mass energies of 161 and 172 GeV, respectively. Details of these data samples, including definition of the criteria imposed for track selection and lepton identification, and a description of the luminosity measurements, have been given in [9,15]. A detailed description of the DELPHI detector may be found in [16], which includes descriptions of the main components of the detector used in this study, namely, the trigger system, the luminosity monitor, the tracking system in the barrel and forward regions, the muon detectors and the electromagnetic calorimeters.

2.1 Selection of events for the study of WWV couplings

In the determination of WWV couplings, events were selected from topologies populated by the production and decay of a WW pair, and from those containing the products of single W production.

Pair production of Ws populates three final state topologies, depending on the decay mode of each W: the topology in which one W decays leptonically and the other hadronically ($jj\ell\nu$), in which two hadronic jets and an isolated lepton are reconstructed, the fully hadronic topology ($jjjj$), requiring the presence of four hadronic jets, and the topology containing only two identified leptons coming from the interaction point ($\ell\nu\ell\nu$).

Single W production in the reaction $e^+e^-\to We\nu$ contributes significantly in the kinematic region where a final state electron or positron is emitted at small angle to the beam and is thus likely to remain lost in the beam pipe. Depending on the decay mode of the W, this process populates two final state topologies, that with two jets and missing energy (jjX) and that containing only a single lepton coming from the interaction point, but no other track in the detector (ℓX).

While these final states are topologically distinct, they are all represented by the generic e^+e^- interaction producing four final state fermions, $e^+e^-\to f_1\bar{f}_2f_3\bar{f}_4$. In particular, the topologies $jj\ell\nu$ and jjX contain events in two different kinematic regions of the same four-fermion final state, $q_1\bar{q}_2\ell\nu$. The four-fermion generators EXCALIBUR [17] and GRC4F [18], which take account of background diagrams and interference effects coherently, were used to produce simulated events. These generators were interfaced to the JETSET hadronization model [19], tuned to Z^0 data [20], and to the full DELPHI simulation program [16]. Samples of events were generated with both Standard Model and non-Standard Model values of TGC parameters, and were used both to determine the efficiency of the selection criteria in the topologies studied, and to check the accuracy of the analysis procedures in deriving the value of TGC parameters used in the generation of events. In addition, in the analysis of the $jj\ell\nu$ final state, the ERATO generator [21] was used in conjunction with a fast simulation of the DELPHI detector (which included realistic efficiencies and smearing of generated quantities). Cross-checks were made to ensure that the fast and full simulations agreed in the distributions of the kinematic variables used in the analysis. The study of the backgrounds due to $q\bar{q}(\gamma)$ and ZZ production was made using fully simulated events generated with the PYTHIA program [22].

Each topology was selected as described below.

$jj\ell\nu$:

Events in the $jj\ell\nu$ topology are characterized by two hadronic jets, one isolated electron or muon (coming either from W decay or from the cascade decay $W\to\tau...\to\ell...$) or a low multiplicity jet with only one charged particle, due to τ decay, and missing momentum resulting from the neutrino. The major background comes from $q\bar{q}(\gamma)$ production and from four-fermion final states containing two quarks and two leptons of the same flavour. The criteria used to select such events from the 161 and 172 GeV data samples have been defined in [9] and [15] for the two energies respectively. At 161 GeV, 12 events were selected with an efficiency, averaged over the three leptonic channels, of $(60.9 \pm 3.0)\%$ and an estimated background of 1.9 ± 0.2 events; at 172 GeV, 40 events were selected (17 $jj\mu\nu$, 14 $jje\nu$ and 9 $jj\tau\nu$), the average efficiency was $(67.2 \pm 1.5)\%$ and a background contamination of 3.6 ± 0.4 events was estimated. A 6-constraint kinematic fit was then applied to the 172 GeV data, imposing 4-momentum conservation, requiring both W masses to be equal to 80.35 GeV/c^2 and requiring the χ^2 probability of the fit to exceed 0.001. This resulted in a sample of 34 events (15 $jj\mu\nu$, 12 $jje\nu$ and 7 $jj\tau\nu$) with average efficiency of $(62.6\pm1.5)\%$ and an estimated background contamination of 1.9 ± 0.3 events.

$jjjj$:

The criteria used to define the sample of events in the $jjjj$ topology at 161 GeV have been given in [9]. In this procedure, events were forced to a four-jet configuration. A variable D was defined as $D = \frac{E_{min}}{E_{max}}\theta_{min}/(E_{max} - E_{min})$, where E_{min} and E_{max} are the energies of the jets with minimum and maximum energy and θ_{min} is the minimum interjet angle. The dominant background, which arises from the $q\bar{q}\gamma$ final state, was suppressed by imposing the condition $D > 0.013$ GeV^{-1}. At 172 GeV, the requirement on D was replaced by a condition on the three eigenvalues, $\mathcal{P}_{1..3}$, of the momentum tensor which, when normalized such that their sum is unity, each have an expectation value of 1/3: the product $27 \cdot \mathcal{P}_1\mathcal{P}_2\mathcal{P}_3$ was required to exceed 0.025. In addition, at least one of the three 5-constraint kinematic fits which could be made to the event, imposing equality of two di-jet masses, was required to have $\chi^2 < 50$. The selected $jjjj$ samples consisted of 15 events at 161 GeV and 52 events at 172 GeV, with estimated background contamination of 5.5 ± 0.6 and 15.2 ± 1.0 events, respectively. The efficiencies for reconstructing events in the kinematically accepted region were found to be $(69 \pm 3)\%$ at 161 GeV and $(71 \pm 2)\%$ at 172 GeV.

$\ell\nu\ell\nu$:

Events in the $\ell\nu\ell\nu$ topology were selected from events with multiplicity less than 5 and which satisfied a 2-jet description, thus allowing decays into τ leptons as well as into μ and e to be included. Requirements on the minimum polar angle of the jets relative to the beam axis and on the direction of the missing momentum helped to suppress the dominant backgrounds, which are from $e^+e^-\to Z(\gamma)$, Bhabha scattering and two-photon collisions. The criteria used at 161 and 172 GeV are described in [9] and [23], respectively. They resulted in the selection of 2 events at 161 GeV and 7 events at 172 GeV, with estimated efficiencies of $(48 \pm 3)\%$ and $(55 \pm 1)\%$ and background contamination of 0.6 ± 0.4 and 1.9 ± 0.5 events at the two energies, respectively.

jjX:

The selection of events in the single W channel jjX was devised so as to accept events which could be interpreted in terms of two jets and missing momentum, but to reject events from the $q\bar{q}(\gamma)$ final state, in which the missing momentum is expected to lie near the beam direction. This reaction constitutes the principal background in the selection of

jjX events, but with a cross-section which is falling with increasing centre-of-mass energy. Events were reconstructed with the LUCLUS algorithm [19] with $d_{\rm join} = 5.5$ GeV/c and those with 2 or 3 jets were forced into a 2-jet configuration. Cuts were then applied on the energy of each jet ($E_j > 20$ GeV at 161 GeV, $E_j > 10$ GeV at 172 GeV), on the jet polar angles relative to the beam axis ($25^\circ < \theta_{jet} < 155^\circ$ at 161 GeV, $15^\circ < \theta_{jet} < 165^\circ$ at 172 GeV), on the di-jet invariant mass ($m_{jj} > 45$ GeV/c^2 at 161 GeV, $m_{jj} > 50$ GeV/c^2 at 172 GeV), on the angle between the direction of the missing momentum and the beam direction ($|\cos\theta_{miss}| < 0.9$), and on the acollinearity angle of the jets and on their acoplanarity with respect to the beam direction ($\theta_{acol} < 165^\circ$, $\theta_{acop} > 11^\circ$ at 161 GeV, $\theta_{acol} < 168.5^\circ$, $\theta_{acop} > 11.5^\circ$ at 172 GeV). Events were rejected if there was an energy deposition cluster of greater than 15 GeV in the electromagnetic calorimeter, isolated from the nearest charged particle by more than 20°. Application of these procedures led to the selection of 6 events at 161 GeV and 8 events at 172 GeV. Efficiencies of $(83 \pm 3)\%$ and $(88 \pm 4)\%$ were estimated in the selected kinematic region, leading to expected signal rates of 1.4 and 3.0 events for Standard Model values of the couplings and backgrounds of 5.5 ± 0.6 and 6.2 ± 0.7 events at the two energies, respectively.

ℓX:
In the selection of events in the ℓX topology, candidate events were required to have only one charged particle track, clearly identified as a muon or electron (tau events were not used). The normal track selections were tightened in order to reject cosmic ray background: the track was required to pass within 1 cm of the interaction point in the xy plane (perpendicular to the beam) and within 4 cm in z. Lepton candidates were also required to have momentum $p < 75$ GeV/c, with transverse component $p_t > 20$ GeV/c. Efficiencies of $(94 \pm 2)\%$ and $(81 \pm 3)\%$ in the selected kinematic region were estimated at both 161 and 172 GeV for muon and electron events, respectively, and the background was estimated to be negligible. One muon event was selected at each of the two energies while, for Standard Model values of the couplings, 0.7 and 0.8 events were expected at each energy, respectively.

2.2 Selection of events for the study of $ZV\gamma$ couplings

The study of $ZV\gamma$ couplings in the reaction $e^+e^- \to \nu\bar{\nu}\gamma$ involved a search for events containing only a single photon of high energy, emitted at large angle θ to the beam direction. Such events were selected by requiring the presence of a "good quality shower" (defined in [16]) of energy $E_\gamma > 25$ GeV in the angular region $45^\circ < \theta < 135^\circ$, covered by the barrel electromagnetic calorimeter. Events with a signal in the forward electromagnetic calorimeter were rejected, and a second shower in the barrel calorimeter was accepted only if it was within 20° of the first one. Events were also rejected if any charged particles were detected in the time projection chamber, the main tracking device of DELPHI, or in the forward tracking chambers. The presence of charged particles not pointing to the nominal beam crossing point also caused events to be rejected; this suppressed background from beam gas interactions and cosmic ray events. In order to reject the background from radiative Bhabha and Compton events, no energy deposit was allowed in the luminosity monitor, situated in the very forward direction. A further rejection of cosmic ray events was achieved by imposing a constraint on the photon direction: the line of flight and the shower direction measured in the calorimeter were required to coincide within 15°. Application of these criteria produced samples of 8 events at 161 GeV and 7 events at 172 GeV.

In order to estimate the cross-section for the single photon production process, the trigger and identification efficiencies must be known. The former was measured using radiative events ($\mu^+\mu^-\gamma$ and $e^+e^-\gamma$) and Compton events. The identification efficiency was estimated using samples of 2500 fully simulated events at each energy, produced with the generator NUNUGPV [24]. The overall efficiency was shown to be dependent on the photon energy in the angular region under consideration, ranging from 58% at $E_\gamma = 25$ GeV to $\geq 71\%$ for $E_\gamma > 50$ GeV. Possible sources of background to the single photon production process include the QED processes $e^+e^- \to \gamma e^+e^-$ and $e^+e^- \to \gamma\gamma$, $\gamma\gamma$ collisions, cosmic ray and Compton events, and beam gas interactions. All of these were found to give negligible contributions.

3 Results on WWV couplings

From the results of previous studies [1], it is expected that the data in the $jj\ell\nu$ topology at 172 GeV will provide the greatest precision in the determination of WWV couplings. These data were analyzed by studying the joint distribution of two variables which retain all the available information of the 7-dimensional phase space describing the four-particle final state. These "Optimal Variables" [25] are derived from the formalism of optimal observables [26] which has been applied to TGC determination in [1,27]. Results using this method are compared below with those using distributions of well-measured variables, namely the production angle of the W^- with respect to the electron beam, θ_W, and the polar angle of the lepton in the laboratory frame, θ_l. In addition, information obtained from the total numbers of events observed in the $jjjj$ and $\ell\nu\ell\nu$ channels, and data from the single W topologies jjX and ℓX, were used to obtain overall results from the 172 GeV data. Results from the same topologies at 161 GeV, using information from the distributions of θ_W and θ_l in the $jj\ell\nu$ final state, were combined with those at 172 GeV to give final values for the couplings.

The analysis using the method of Optimal Variables exploits the fact that the differential cross-section, $d\sigma/d\vec{V}$, where $\vec{V}$ represents the phase space variables, is quadratic in TGC parameters: $d\sigma(\vec{V},\vec{\alpha})/d\vec{V} = c_0(\vec{V}) + \sum_i \alpha_i c_1^i(\vec{V}) + \sum_{ij} \alpha_i\alpha_j c_2^{ij}(\vec{V})$, where the sums are over the set $\vec{\alpha} \equiv \alpha_1 ... \alpha_N$ of parameters under consideration. In the case of the determination of single parameters α considered in this paper, the right-hand side of the above expression is a simple quadratic expansion in α: $d\sigma(\vec{V},\alpha)/d\vec{V} = c_0(\vec{V}) + \alpha c_1(\vec{V}) + \alpha^2 c_2(\vec{V})$. In [25] it is shown that the distribution in the 2-variable space of $c_1(\vec{V})/c_0(\vec{V})$ and $c_2(\vec{V})/c_0(\vec{V})$ retains the whole information carried by the full distribution $d\sigma/d\vec{V}$ and hence allows the determination of α with maximum precision, equivalent to that of a maximum likelihood fit over all the phase space variables. Furthermore, it is argued and confirmed by tests on simulated events that little loss of precision occurs if the phase space variables $\vec{\Omega}$ available after reconstruction of events from experimental data are used in place of the true variables $\vec{V}$.

The sample of 34 $jj\ell\nu$ events at 172 GeV was analyzed by performing a binned extended maximum likelihood fit to the two-dimensional distribution of $c_1(\vec{\Omega})/c_0(\vec{\Omega})$ and $c_2(\vec{\Omega})/c_0(\vec{\Omega})$ for each of the parameters $\alpha_{W\phi...}$ defined in section 1, keeping the others fixed to their Standard Model values of zero. The expected numbers of events were computed for several values of the couplings using the ERATO four-fermion generator and a full simulation of the DELPHI detector. A reweighting technique was then used to estimate the expected cross-section in each bin as a continuous function of each parameter fitted. Results on the CP-conserving TGC parameters $\alpha_{W\phi}$, α_W and $\alpha_{B\phi}$ are shown in the

first column of table 1. Figures 1a) and b) show the distributions of $c_1(\vec{\Omega})/c_0(\vec{\Omega})$ and $c_2(\vec{\Omega})/c_0(\vec{\Omega})$, respectively, together with the expected distributions for the fitted value of one TGC parameter, $\alpha_{W\phi}$. The validity of the technique was verified by applying it to a large number of samples of fully simulated events corresponding to the same integrated luminosity as the data, generated both with Standard Model and non-Standard Model values of the couplings. The mean values of the precisions in the TGC parameters obtained from these samples were found to be compatible with those from the data, and the pull distributions had means and variances compatible with 0 and 1, respectively.

TGC parameter	Topologies used			
	$jj\ell\nu$ (Optimal Variables)	$jj\ell\nu$ ($\cos\theta_W$, $\cos\theta_\ell$)	$jj\ell\nu + jjjj$ $+\ell\nu\ell\nu$	$jj\ell\nu + jjjj$ $+\ell\nu\ell\nu + jjX + \ell X$
$\alpha_{W\phi}$	$0.38^{+0.32}_{-0.32}$	$0.61^{+0.42}_{-0.49}$	$0.35^{+0.28}_{-0.39}$	$0.30^{+0.28}_{-0.30}$
α_W	$0.28^{+0.57}_{-0.57}$	$0.91^{+0.59}_{-0.74}$	$0.26^{+0.50}_{-0.53}$	$0.24^{+0.45}_{-0.53}$
$\alpha_{B\phi}$	$1.45^{+1.12}_{-1.47}$	$1.74^{+1.20}_{-2.67}$	$1.27^{+0.99}_{-1.39}$	$0.24^{+0.85}_{-0.93}$

Table 1: Results obtained from fits to CP-conserving WWV coupling parameters at 172 GeV using various analysis procedures and data from various final state topologies. Values shown in the third and fourth columns have been obtained by combining the $jj\ell\nu$ results in the first column with data from additional topologies. In each fit, the values of the other TGC parameters were kept at their Standard Model values.

These results may be compared with those obtained from an analysis of the joint distribution in $(\cos\theta_W, \cos\theta_\ell)$. These quantities can be directly estimated without serious bias from the sum of the two measured hadronic jet vectors and the direction of the observed lepton. Using the sample of $jj\ell\nu$ events obtained before application of a kinematic fit, the binned distribution in the $(\cos\theta_W, \cos\theta_\ell)$ plane was fitted to that predicted using ERATO and a fast simulation of the detector response; the results are shown in the second column of table 1. They are in agreement with those from the Optimal Variables analysis, though, as expected, with lower precision. The distributions of these variables are shown in figures 1c) and d) together with the expected distributions for the fitted value of $\alpha_{W\phi}$. Further analyses of the distributions in these variables using different four-fermion generators [18,28] have given results in agreement with those shown in the table.

The third and fourth columns of table 1 show the increase in precision obtained in the CP-conserving TGC parameters at 172 GeV by addition to the results obtained from the Optimal Variables analysis of the $jj\ell\nu$ channel, first, of data from the $jjjj$ and $\ell\nu\ell\nu$ final states, then from the single W topologies jjX and ℓX. For the $jjjj$ and $\ell\nu\ell\nu$ topologies, the observed total numbers of events were compared with those expected as a function of each TGC parameter. In the analysis of the jjX final state, the differential distribution in $|\cos\theta_W|$, estimated from the sum of the two reconstructed jet momenta, was also used. The GRC4F generator was used for the calculation of the expected number of events, and fully simulated samples of events generated with EXCALIBUR at values of -2.0, 0.0 and +2.0 for each parameter were used to estimate the detector response. In general, a modest increase in precision is seen as results from each new data set are added.

Because the contributions to the amplitude for WW production from diagrams with s-channel γ and Z exchange contain a factor proportional to the W velocity, the sensitivity

of the data to TGC parameters at 161 GeV is considerably smaller than at 172 GeV. Nonetheless, differential data ($\cos\theta_W$, $\cos\theta_\ell$) from $jj\ell\nu$ events, the total numbers of events observed in the $jjjj$ and $\ell\nu\ell\nu$ final states, the distribution of $|\cos\theta_W|$ from jjX events and the number of events in the ℓX final state at 161 GeV have been used to supplement the results obtained from the higher energy data. Results obtained for both CP-conserving and CP-violating couplings are shown for each of these energies in the first two columns of table 2, together with their statistical errors.

TGC parameter	161 GeV	172 GeV	161 + 172 GeV
$\alpha_{W\phi}$	$-0.27^{+0.74}_{-0.70}$	$0.30^{+0.28}_{-0.30}$	$0.22^{+0.25}_{-0.28} \pm 0.06$
α_W	$-0.90^{+1.40}_{-0.98}$	$0.24^{+0.45}_{-0.53}$	$0.11^{+0.48}_{-0.49} \pm 0.09$
$\alpha_{B\phi}$	$0.18^{+0.98}_{-2.70}$	$0.24^{+0.85}_{-0.93}$	$0.22^{+0.66}_{-0.83} \pm 0.24$
$\tilde{\alpha}_{BW}$	$0.72^{+0.77}_{-2.20}$	$0.02^{+0.80}_{-0.77}$	$0.11^{+0.71}_{-0.88} \pm 0.09$
$\tilde{\alpha}_W$	$-0.54^{+1.31}_{-0.40}$	$0.19^{+0.28}_{-0.38}$	$0.19^{+0.28}_{-0.41} \pm 0.11$

Table 2: Results obtained from fits to WWV coupling parameters. The first two columns show the values obtained from the 161 GeV and 172 GeV data with their statistical errors. The third column shows the combined results; the first error is statistical, the second is systematic (see table 3 below for details). In each fit, the values of the other TGC parameters were kept at their Standard Model values.

Various systematic effects were considered and the estimated errors incurred in the fitted TGC parameters are given in detail for the 172 GeV data and summarized for the 161 GeV data in table 3. The table contains contributions arising from a conservatively estimated precision of ± 100 MeV/c^2 in the value of the W mass [29], from the uncertainty in the LEP beam energy [30] and experimental luminosity, from the theoretical uncertainty in the cross-section evaluation (taken to be $\pm 2\%$ [1]), from the errors in the estimated signal and background cross-sections due to limited simulated statistics and, in the $jj\ell\nu$ final state, from the granularity of the binning used in the fits and from uncertainties in the detector response which could affect the differential distributions, as described in [15]. The systematic error due to the use of a different hadronization algorithm in jet reconstruction was also computed and found to be small compared to those quoted in the table. The combined effect of all contributions to the systematic uncertainty at 161 GeV is also shown.

The third column of table 2 shows the final results for the TGC parameters, obtained by combining the results at 161 and 172 GeV, together with their statistical and systematic errors. The systematic errors were obtained by adding in quadrature the first four contributions in table 3, considered as common to all topologies and to both energies, and combining the result with the non-common contributions, which were each weighted with the statistical precision of the topology concerned. The log likelihood distributions from which the results are derived are shown in figure 2. The parameter values determined are all consistent with zero, and hence with the expectations of the Standard Model.

	$\alpha_{W\phi}$	α_W	$\alpha_{B\phi}$	$\tilde{\alpha}_{BW}$	$\tilde{\alpha}_W$
Common systematics:					
W mass	0.02	0.03	0.08	0.02	0.04
E_{cm}	0.02	0.02	0.04	0.02	0.02
Cross-section	0.03	0.04	0.16	0.03	0.06
Luminosity	0.01	0.01	0.05	0.01	0.02
Topology $jj\ell\nu$, 172 GeV:					
Binning granularity	0.02	0.03	0.04	0.03	0.03
Signal estimation	0.02	0.03	0.12	0.02	0.04
Background estimation	0.01	0.02	0.06	0.01	0.02
Topologies $jjjj + \ell\nu\ell\nu$, 172 GeV:					
Signal estimation	0.04	0.05	0.06	0.04	0.04
Background estimation	0.03	0.03	0.04	0.03	0.03
Topologies $jjX + \ell X$, 172 GeV:					
Signal estimation	0.03	0.10	0.04	0.00	0.01
Background estimation	0.09	0.21	0.13	0.00	0.02
Combined systematics, 172 GeV:					
	0.03	0.07	0.12	0.05	0.05
Combined systematics, 161 GeV:					
	0.07	0.10	0.15	0.15	0.30

Table 3: Estimated systematic uncertainties in the determination of WWV coupling parameters. Details of the common and topology-dependent contributions are shown for 172 GeV data; the total of all non-common contributions is summarized for 161 and 172 GeV data. The entries for the $jj\ell\nu$ topology at 172 GeV refer to the analysis based on Optimal Variables, described in the text.

4 Results on $ZV\gamma$ couplings

The sample of 15 events selected from the combined data at 161 and 172 GeV yields a cross-section

$$\sigma(e^+e^- \to \gamma \ + \ \text{invisible particles}) = 1.47 \pm 0.38(\text{stat.}) \pm 0.30(\text{syst.}) \ \text{pb}$$

in the region of phase space with $E_\gamma > 25$ GeV and $45^\circ < \theta_\gamma < 135^\circ$, corrected for the experimental efficiencies within these selections. The systematic uncertainty comes mainly from the calibration of the calorimeter energy scale and from the errors on the detection and trigger efficiencies.

The cross-section given above corresponds to a 95% C.L. limit

$$\sigma(e^+e^- \to \gamma \ + \ \text{invisible particles}) < 2.5 \ \text{pb}$$

in the same region of phase space, including the effect of systematic uncertainties. This limit is shown in figure 3 together with the predicted cross-section as a function of the $ZV\gamma$ coupling parameters h^{γ}_{30} and h^{Z}_{30} defined in section 1. Limits at 95% C.L. of

$$|h^{\gamma}_{30}| < 0.8 \qquad \text{and} \qquad |h^{Z}_{30}| < 1.3$$

are derived at a scale $\Lambda = 1$ TeV and with $n = 3$ in the form factor representation of h^{V}_{3}. The limit obtained for $|h^{\gamma}_{30}|$ represents a considerable improvement over those reported previously from LEP data [13,14], and may be compared with the current limit set by the D0 experiment: $|h^{\gamma}_{30}| < 0.37$ for $\Lambda = 750$ GeV [12]. The limit obtained for $|h^{Z}_{30}|$ exceeds the unitarity limit, $|h^{Z}_{30}| = 0.99$, for the values of Λ and n used in the form factor, and for current values of $\sqrt{s}$, the data show little sensitivity to the other CP-conserving vertex factors, h^{V}_{4}. If the analysis is applied to measure the CP-violating parameters h^{γ}_{10} and h^{Z}_{10}, the same limits are obtained as for h^{V}_{30}.

5 Conclusions

Trilinear gauge couplings have been measured in DELPHI using data corresponding to integrated luminosities of 10.0 pb^{-1} at 161 GeV and 9.98 pb^{-1} at 172 GeV. Values of the CP-conserving WWV couplings $\alpha_{W\phi}$, α_{W} and $\alpha_{B\phi}$ and of the CP-violating couplings $\tilde{\alpha}_{BW}$ and $\tilde{\alpha}_{W}$ have been derived using data from topologies populated both by WW production, $e^{+}e^{-} \rightarrow W^{+}W^{-}$, and by single W production, $e^{+}e^{-} \rightarrow We\nu$. The results are summarized in table 2. Limits on the $ZV\gamma$ couplings $h^{\gamma,Z}_{3}$ have also been determined using data from single photon production, with results given in section 4. No evidence for deviations from Standard Model predictions is observed in the present data. Further running at LEP2 should yield an improvement of up to an order of magnitude in the precision of the results obtained.

Acknowledgements

We thank the SL division of CERN for the excellent performance of the LEP collider and their careful work on the beam energy determination. We are also grateful to the technical and engineering staffs in our laboratories and to our funding agencies for their continuing support.

References

[1] G. Gounaris, J.-L. Kneur and D. Zeppenfeld, in *Physics at LEP2*, eds. G. Altarelli, T. Sjöstrand and F. Zwirner, CERN 96-01 Vol.1, 525 (1996).

[2] G. Gounaris and C.G. Papadopoulos, *Studying Trilinear Gauge Couplings at Next Linear Collider*, DEMO-HEP-96/04, THES-TP 96/11, hep-ph/9612378 (1996).

[3] G. Borisov, V.N. Larin and F.F. Tikhonin, Z. Phys. **C41** (1988) 287;
D. Choudhury and J. Kalinowski, Nucl. Phys. **B491** (1997) 129.

[4] U. Baur and E. L. Berger, Phys. Rev. **D47** (1993) 4889.

[5] H. Aihara *et al.*, *Anomalous Gauge Boson Interactions*, FERMILAB-Pub-95/031, MAD/PH/871, UB-HET-95-01, UdeM-GPP-TH-95-14, hep-ph/9503425 (1995).

[6] T. Yasuda, *Tevatron Results on Gauge Boson Couplings*, FERMILAB-Conf-97/206-E, to appear in the proceedings of the Hadron Collider Conference XII, Stony Brook, hep-ex/9706015 (1997).

[7] CDF Collaboration, F. Abe *et al.*, Phys. Rev. Lett. **74** (1995) 1936;
CDF Collaboration, F. Abe *et al.*, Phys. Rev. Lett. **78** (1997) 4536;
D0 Collaboration, S. Abachi *et al.*, Phys. Rev. Lett. **78** (1997) 3634.

[8] D0 Collaboration, S. Abachi *et al.*, Phys. Rev. **D56** (1997) 6742.

[9] DELPHI Collaboration, P. Abreu *et al.*, Phys. Lett. **B397** (1997) 158.

[10] OPAL Collaboration, K. Ackerstaff *et al.*, Phys. Lett. **B397** (1997) 147;
OPAL Collaboration, K. Ackerstaff *et al.*, *Measurement of triple gauge boson couplings from* W^+W^- *production at* $\sqrt{s}$ *= 172 GeV*, CERN-PPE/97-125 (1997);
L3 Collaboration, M. Acciarri *et al.*, Phys. Lett. **B398** (1997) 223;
L3 Collaboration, M. Acciarri *et al.*, Phys. Lett. **B403** (1997) 168;
L3 Collaboration, M. Acciarri *et al.*, Phys. Lett. **B413** (1997) 176.

[11] CDF Collaboration, F. Abe *et al.*, Phys. Rev. Lett. **74** (1995) 1941.

[12] D0 Collaboration, B. Abbott *et al.*, $Z\gamma$ *Production in* $p\bar{p}$ *Collisions at* $\sqrt{s}$ = 1.8 *TeV and Limits on Anomalous* $ZZ\gamma$ *and* $Z\gamma\gamma$ *Couplings*, Fermilab-Pub-97/363-E, hep-ex/9710031 (1997), submitted to Phys. Rev. Lett.

[13] L3 Collaboration, M. Acciarri *et al.*, Phys. Lett. **B346** (1995) 190.

[14] DELPHI Collaboration, P. Abreu *et al.*, Phys. Lett. **B380** (1996) 471.

[15] DELPHI Collaboration, P. Abreu *et al.*, *Measurement of the W-pair cross-section and of the W mass in* e^+e^- *interactions at 172 GeV*, CERN-PPE/97-160 (1997).

[16] DELPHI Collaboration, P. Abreu *et al.*, Nucl. Inst. Meth. **A378** (1996) 57.

[17] F.A. Berends, R. Kleiss and R. Pittau, *EXCALIBUR*, in *Physics at LEP2*, eds. G. Altarelli, T. Sjöstrand and F. Zwirner, CERN 96-01 Vol.2, 23 (1996).

[18] J. Fujimoto *et al., GRC4F*, in *Physics at LEP2*, eds. G. Altarelli, T. Sjöstrand and F. Zwirner, CERN 96-01 Vol.2, 23 (1996).

[19] T. Sjöstrand, *PYTHIA 5.7 / JETSET 7.4*, CERN-TH.7112/93 (1993).

[20] DELPHI Collaboration, P. Abreu *et al.*, Z. Phys. **C73** (1996) 11.

[21] C.G. Papadopoulos, Comp. Phys. Comm. **101** (1997) 183.

[22] T. Sjöstrand, *PYTHIA 5.719 / JETSET 7.4*, in *Physics at LEP2*, eds. G. Altarelli, T. Sjöstrand and F. Zwirner, CERN 96-01 Vol.2, 41 (1996).

[23] T. Bowcock *et al.*, *Measurement of Trilinear Gauge Couplings in* e^+e^- *Collisions at 161 GeV and 172 GeV*, DELPHI note 97-113, CONF 95, submitted to the EPS HEP97 Conference, Jerusalem (August 1997).

[24] G. Montagna *et al.*, Nucl.Phys. **B452** (1996) 161.

[25] G.K. Fanourakis, D. Fassouliotis and S.E. Tzamarias, *Accurate Estimation of the Trilinear Gauge Couplings Using Optimal Observables Including Detector Effects*,

DEMO-HEP 97/09, hep-ex/9711015 (1997).
[26] M. Diehl and O. Nachtmann, Z. Phys. **C62** (1994) 397.
[27] C.G. Papadopoulos, Phys. Lett. **B386** (1996) 442;
M. Diehl and O. Nachtmann, *Anomalous three Gauge Couplings in* $e^+e^- \to W^+W^-$ *and 'Optimal' Strategies for their Measurement*, HD-THEP-97-03, CPTH-S494-0197, hep-ph/9702208 (1997).
[28] G. Montagna, O. Nicrosini and F. Piccinini, *et al., WWGENPV*, in *Physics at LEP2*, eds. G. Altarelli, T. Sjöstrand and F. Zwirner, CERN 96-01 Vol.2, 23 (1996).
[29] Y.K. Kim, *Precision tests of the Electroweak Interactions from Hadron Colliders*, Talk presented at the Lepton-Photon Symposium, LP97, Hamburg, July 1997.
[30] The working group for LEP energy, *LEP Energy Calibration in 1996*, Lep Energy Group/97-01 (1997).

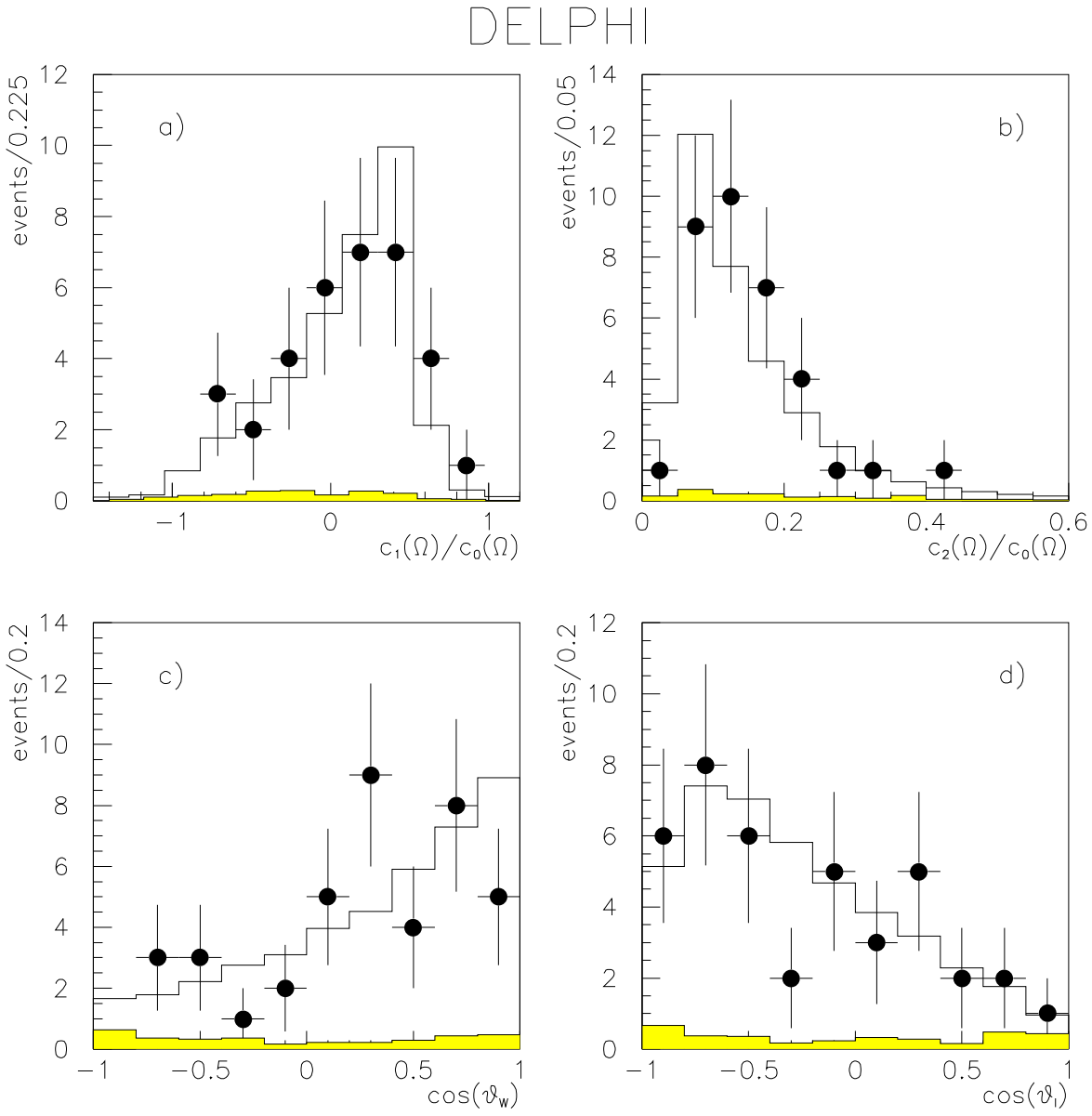

Figure 1: Distributions of pairs of variables used in the fitting of WWV coupling parameters in the $jj\ell\nu$ final state at 172 GeV; a) and b) the Optimal Variables $c_1(\vec{\Omega})/c_0(\vec{\Omega})$ and $c_2(\vec{\Omega})/c_0(\vec{\Omega})$ for $\alpha_{W\phi}$; c) and d) $\cos\theta_W$ and $\cos\theta_\ell$. The points represent the data, and the histograms the expectation for the values of $\alpha_{W\phi}$ shown in table 1 with background contributions shaded.

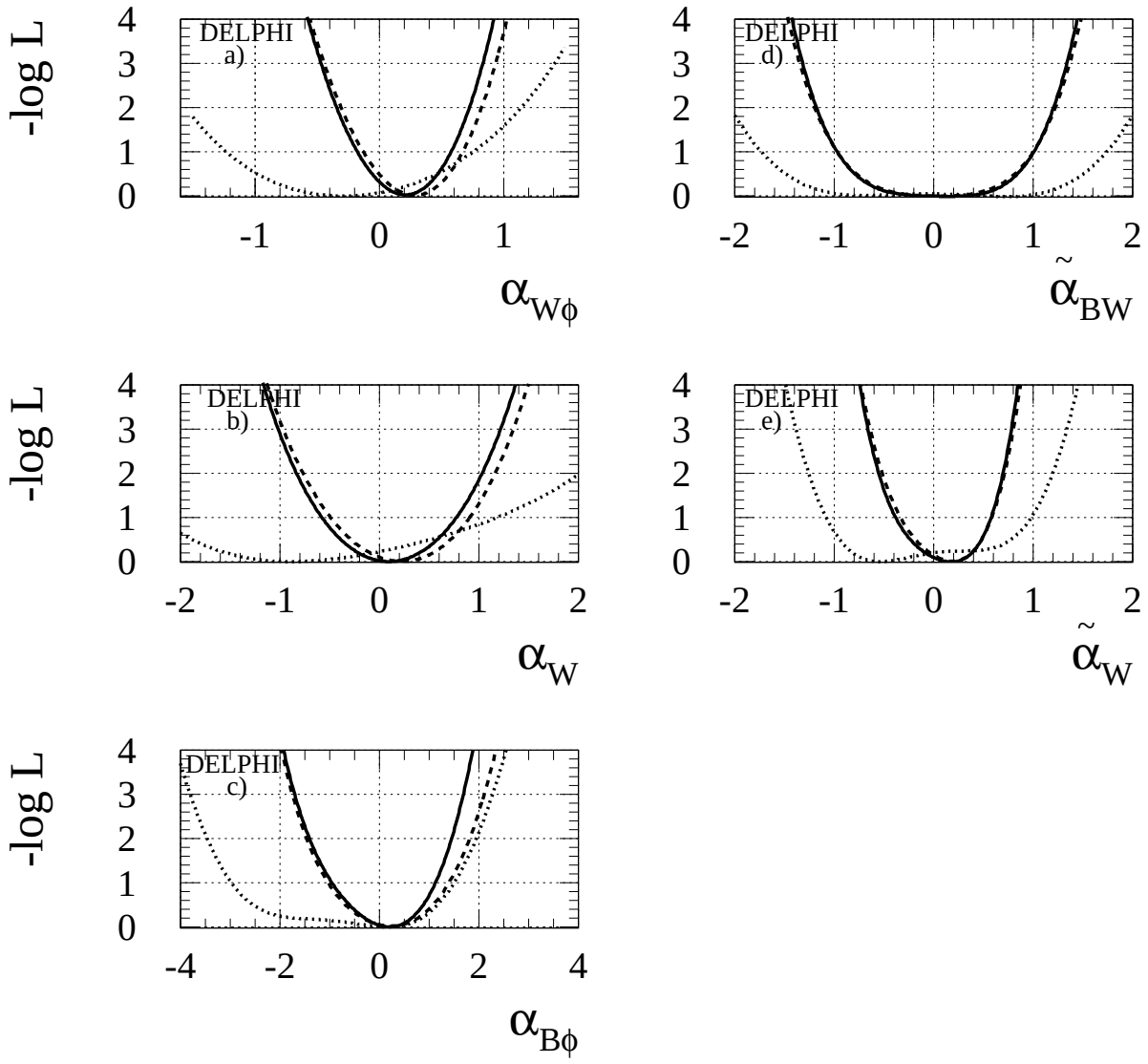

Figure 2: Distributions of log likelihood as a function of WWV coupling parameters; a) $\alpha_{W\phi}$, b) α_W, c) $\alpha_{B\phi}$, d) $\tilde{\alpha}_{BW}$, e) $\tilde{\alpha}_W$. The dotted curves show the functions obtained using data at 161 GeV, the dashed curves are from data at 172 GeV, and the full curves show the results from the two energies combined. In each case, the curves include the effects of statistical and systematic errors.

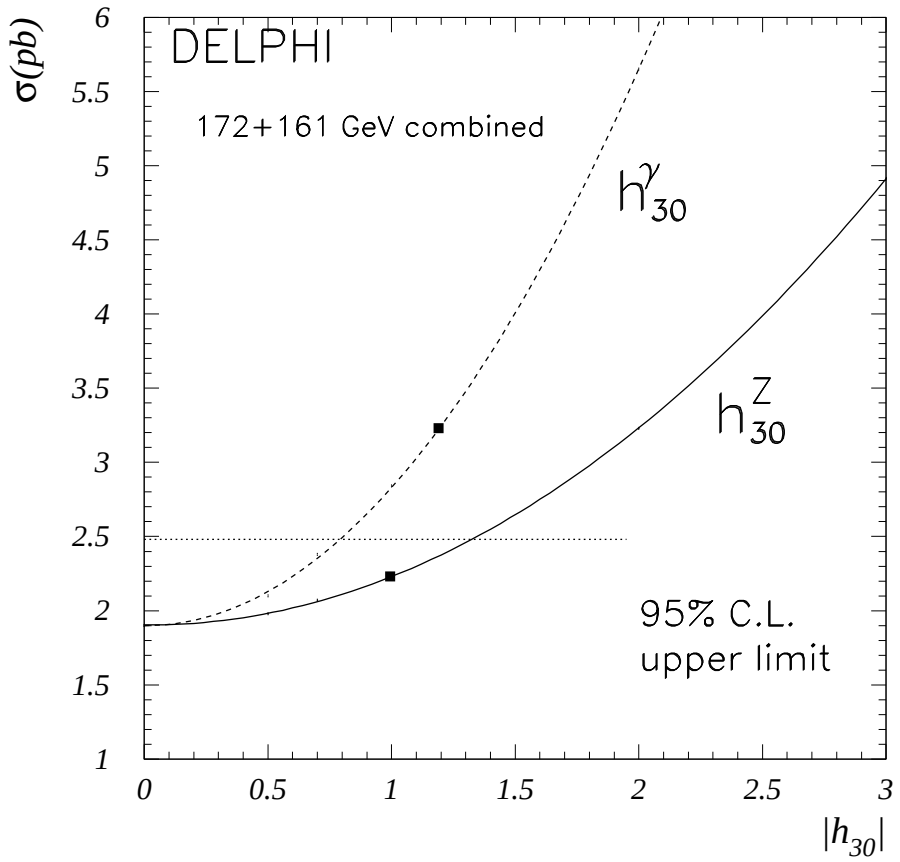

Figure 3: Variation of the predicted cross-section for large angle single photon production in DELPHI at 161 and 172 GeV with the $ZV\gamma$ couplings h_{30}^{γ} and h_{30}^{Z}, for energy scale $\Lambda = 1$ TeV and $n = 3$ in the form factor representation of h_3^V. The square points on the curves show the unitarity limits for the two couplings corresponding to these values of Λ and n.